Electronic Supplementary Information for

Nucleus-staining with biomolecule-mimicking nitrogen-doped carbon dots prepared by fast neutralization heat strategy

Yan-Fei Kang,[a,†] Yang-Wu Fang,[b,†] Yu-Hao Li,[b] Wen Li,[b] and Xue-Bo Yin[a,*]

[a.] Research Center for Analytical Sciences, College of Chemistry, Nankai University, Tianjin Key laboratory of Biosensing and Molecular Recognition, State Key Laboratory of Medicinal Chemical Biology, Collaborative Innovation Center of Chemical Science and Engineering (Tianjin), Tianjin 300071, China.

[b.] Tianjin Key Laboratory of Tumor Microenviroment and Neurovascular Regulation, School of Medicine, Nankai University, Tianjin, 300071, China.

* Correspondence should be addressed to X.B.Y. E-mail: xbyin@nankai.edu.cn; Fax: (+86) 022-23503034

Experimental section

1. Chemicals and materials

Dopamine hydrochloride was purchased from Sigma Aldrich, Shanghai, China. Sodium dihydrogen phosphate (NaH_2PO_4), disodium hydrogen phosphate (Na_2HPO_4), and ethylenediamine were purchased from Tianjin Fuchen Chemical Reagent Factory, Tianjin, China. Phosphoric acid, ethanol and metal ions (Na^+, Pb^{2+}, K^+, Ca^{2+}, Al^{3+}, Fe^{3+}, Mn^{2+}, Zn^{2+}, Mg^{2+}, Co^{2+}, Ni^{2+}, Ag^+ and Cu^{2+}) were bought from Tianjin Fengfan Chemical Technology Co. Ltd., Tianjin, China. Cysteine was bought from Beijing J&K Technology Co. Ltd., Beijing, China. 1640 growth medium was purchased from Gibco. Annexin V-FITC and propidium iodide (PI) were bought from Becton, Dickinson and Company, America. All other reagents used herein were analytically pure. Ultrapure water, 18.25MΩ cm, was produced with Aquapro RM 220 Ultra-purified Water System, Chongqing, China.

2. Instrumentation

Transmission electron microscopy (TEM) images were obtained with Tecnai G^2 F20, FEI Co. (America) operated at an accelerating voltage of 200 kV. X-ray photoelectronic spectroscopy (XPS) analysis was performed with Kratos Axis Ultra DLD (England) fitted with a mono chromatic Al K X-ray source (hν 1486.6 eV), hybrid (magnetic/electrostatic) optics and a multi-channel plate and delay line detector. The fluorescence experiments were carried out by the Hitachi FL-4600 fluorescence spectrometer, Japan. The UV-visible absorption spectrum was recorded by the Shimazu UV-2450 UV-visible spectrophotometer, Japan. Fourier transform infrared (FTIR) spectra were recorded with the Bruker Tensor 27 Fourier transform infrared spectrometer (German). The laser confocal fluorescence images were acquired from the Olympus FV1000 microscope, Japan. The flow cytometry results were measured by flow cytometry (BD LSRFortessa).

3. Synthesis of N-Cdots

N-Cdots were synthesized by one-step neutralization heat method and illustrated in Scheme S1. Briefly, 300 mg dopamine hydrochloride was added into 15 mL ethylenediamine and dissolved ultrasonically. 8 mL phosphoric acid was poured into the ethylenediamine solution quickly and stirred with a glass rod immediately for 2 minutes and then the mixture became light yellow powder. When cooling to room temperature, 25 mL ethanol was added into the mixture and the supernatant was collected after centrifugation at 12000 rpm for 10 min to remove the white salt. Filtrated and then rotary evaporated the supernatant in 60 °C to remove the excess ethylenediamine. N-Cdots were obtained after being purified by dialyzing against deionized water through a dialysis membrane (1000 MW) for 12 h and resulting N-Cdots solution was finally centrifuged at 12000 rpm for 10 min to collect the supernatant. The as-prepared N-Cdots were freeze-dried till powder and stored in the dark for further characterization and use.

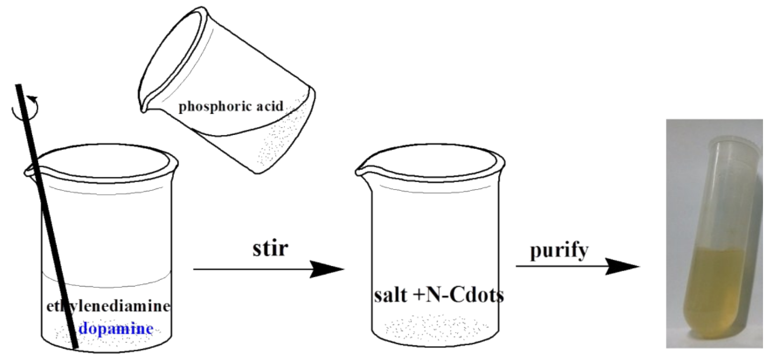

Scheme S1. Schematic representation of fast synthesis of N-Cdots.

4. Cell culture and treatment

PC12, A549, HepG 2 and MD-MBA-231 cells were maintained in 1640 medium supplemented with 10 % fetal bovine serum (FBS) and 1 % penicillin-streptomycin solution (PS) at 37 °C in a humidified atmosphere of 5 % CO_2. The cells were seeded in 24-well culture plates at a density of 1×10^5 cells per well in culture medium and allowed to grow over 12 h (the cells reached 70–80 % confluence). Then the culture medium was replaced by the fresh medium containing N-Cdots with different concentration and kept for certain time.

The PC12 cells in the 24 well tissue plates were washed with PBS for 3 times to remove the N-Cdots in the medium when necessary and sealed the cover slides on the slides with mounting medium to acquire confocal fluorescence images.

When staining the nuclei with DAPI (A549, HepG 2 and MD-MBA-231 cells), the cells were washed with PBS for 3 times to remove the N-Cdots and then add 200 μL DAPI solution (original solution diluted to one thousand times when used) into the 24 well tissue plates and washed with PBS 5 minutes later for 3 times with 10 minutes interval and then sealed the cover slides on the slides with mounting medium to acquire confocal fluorescence images.

5. The confocal fluorescence microscopy equipment

The brightfield and confocal fluorescence images for PC12, A549, HepG 2 and MD-MBA-231 cells were acquired with the Olympus FV1000 microscope (Japan). The green fluorescence images of N-Cdots in cancer cells were acquired under the 488nm excitation light. The blue fluorescence images of nuclei stained with DAPI in cancer cells were acquired under the 405nm excitation light.

6. Detection of Ag^+ ions

Different concentrations of Ag^+ ion solution were added into the N-Cdots solution and the FL spectra were recorded after reaction in the dark for 10 min. The selectivity of N-Cdots for Ag+ was confirmed by adding other metal ion solutions instead of Ag^+ ion solution in a similar way. All experiments were performed at room temperature.

7. Detection of cysteine

500 mM $AgNO_3$ solution was added into the same volume of N-Cdots solution, followed with addition of different concentrations of cysteine solution after reaction in the dark for 10 min. The FL spectra were recorded after the reaction of the mixture for 30 min. The selectivity of the N-Cdots-Ag^+ system for cysteine was confirmed by adding other biological species and analogue solution instead of cysteine solution in a similar way. All experiments were performed at room temperature.

8. Treatment of N-Cdots with boric acid

700 μL different concentrations of boric acid solution (0.5, 1.0, 2.5, 5.0, 10.0, 25.0, 50.0 mM) and ultrapure water acted as control sample were added into 700 μL 0.125 mg mL^{-1} N-Cdots solution (dissolved in 10 mM pH=8.5 PBS). The FL spectra were recorded after the reaction of the mixture for 30 min. All experiments were performed at room temperature.

9. Flow Cytometry

A549 cells were seeded in 6-well culture plates at a density of 2.5×10^5 cells per well in 1640 culture medium added with 10% fetal bovine serum and 1% penicillin-streptomycin solution (PS) at 37 °C in a humidified atmosphere of 5 % CO_2 and allowed to grow over 12 h. After the medium was replaced with fresh culture medium, proper amount of N-Cdots was added into each well to keep the final concentration in the range of 0-1.0 mg mL^{-1} for incubation of 12 h. After rinsing the cells with PBS for three times, the cells were harvested by trypsinization. The cells were resuspended in PBS, then stained with Annexin V-FITC and propidium iodide (PI, final concentration: 1 μg mL^{-1}) and determined by flow cytometry (BD LSRFortessa). The data were analyzed using FlowJo 7.6 software.

Results and discussion

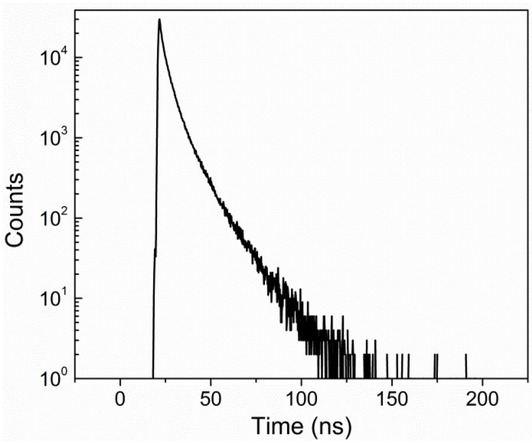

Fig. S1. The fluorescence lifetime spectrum of N-Cdots

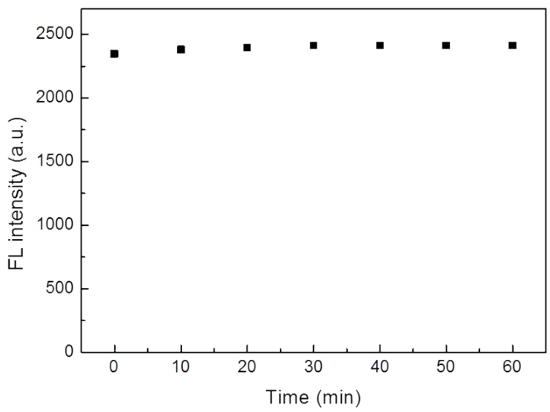

Fig. S2. The fluorescence intensity of N-Cdots on different time points with continuous excitation at 420 nm.

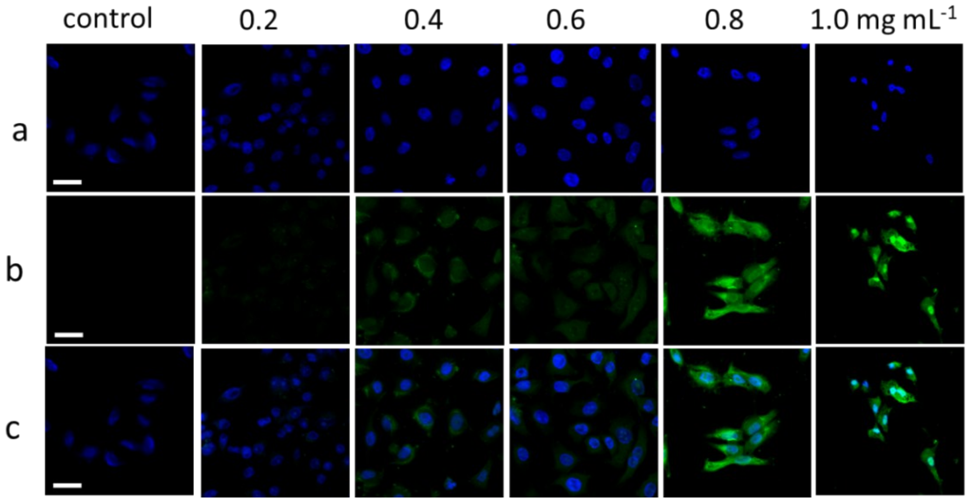

Fig. S3. The confocal fluorescence images of A 549 cell after incubating with medium contains 0, 0.2, 0.4, 0.6, 0.8 and 1.0 mg mL^{-1} of N-Cdots for 12 h: fluorescence images of nucleus stained with DAPI (405 nm excitation and 450–470 nm emission) (a), green fluorescence images of N-Cdots in cells (488 nm excitation and 500–540 nm emission) (b), merge of the fluorescence images of nucleus and N-Cdots in cells (c). Scale bars: 30 μm.

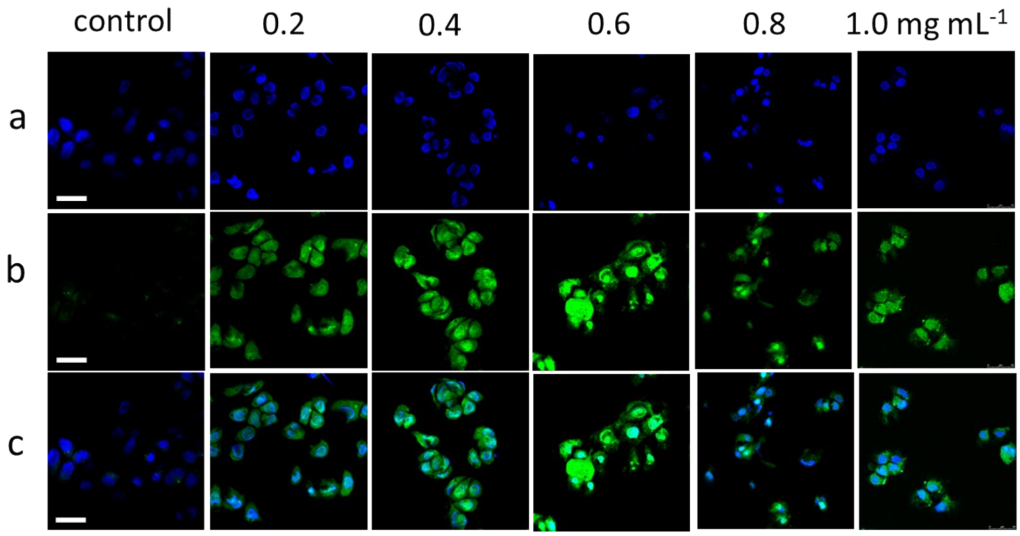

Fig. S4. The confocal fluorescence images of HepG 2 cell after incubating with medium contains 0, 0.2, 0.4, 0.6, 0.8 and 1.0 mg mL^{-1} of N-Cdots for 12 h: fluorescence images of nucleus stained with DAPI (405 nm excitation and 450–470 nm emission) (a), green fluorescence images of N-Cdots in cells (488 nm excitation and 500–540 nm emission) (b) merge of the fluorescence images of nucleus and N-Cdots in cells (c). Scale bars: 30 μm.

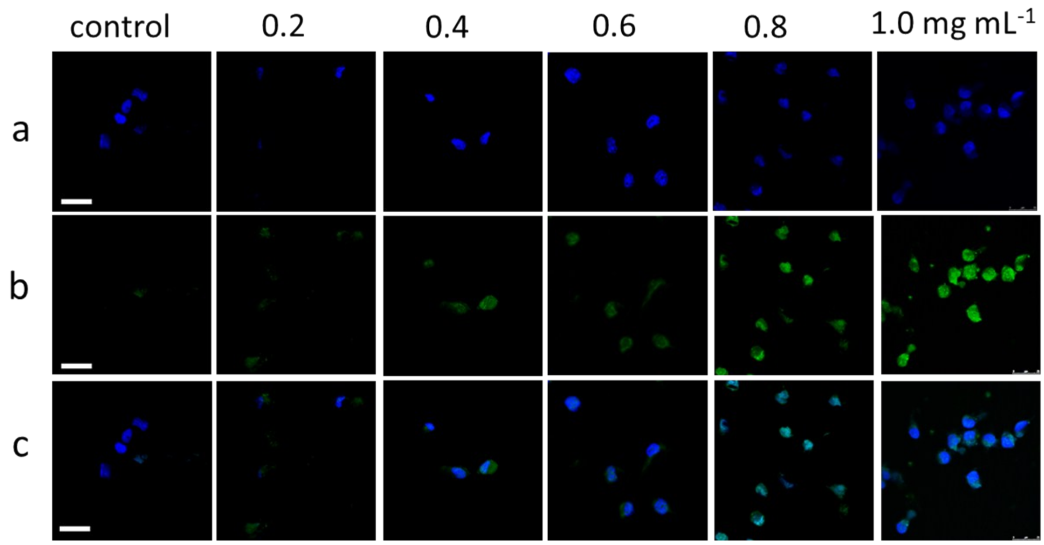

Fig. S5. The confocal fluorescence images of MD-MBA-231 cell after incubating with medium contains 0, 0.2, 0.4, 0.6, 0.8 and 1.0 mg mL^{-1} of N-Cdots for 12 h: fluorescence images of nucleus stained with DAPI (405 nm excitation and 450–470 nm emission) (a), green fluorescence images of N-Cdots in cells (488 nm excitation and 500–540 nm emission) (b) and merge of the fluorescence images of nucleus and N-Cdots in cells (c). Scale bars: 30 μm.

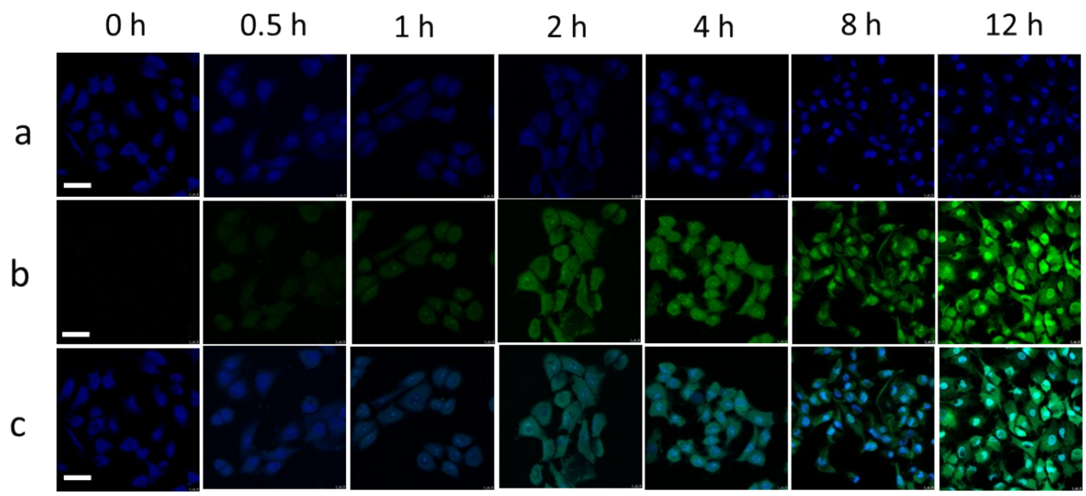

Fig. S6. The confocal fluorescence images of A549 cell after incubating with medium contains 0.8 mg mL^{-1} of N-Cdots for different time: fluorescence images of nucleus stained with DAPI (405 nm excitation and 450–470 nm emission) (a), green fluorescence images of N-Cdots in cells (488 nm excitation and 500–540 nm emission) (b) merge of the fluorescence images of nucleus and N-Cdots in cells (c). Scale bars: 30 μm.

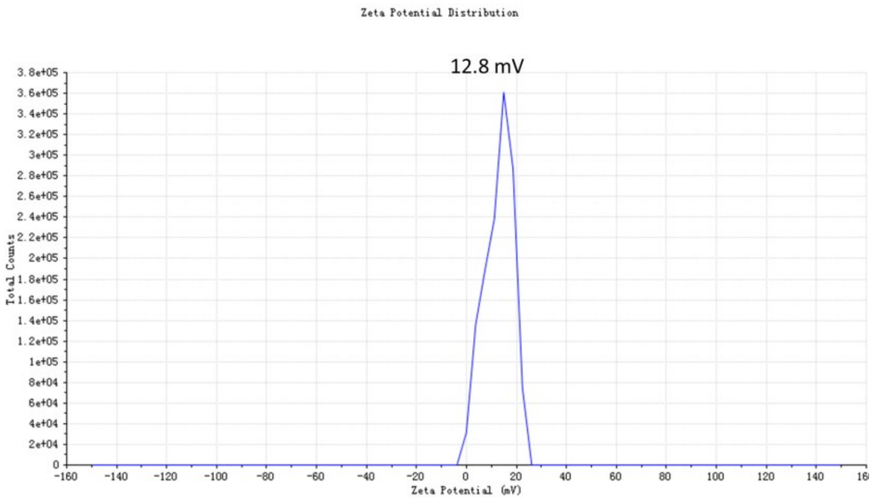

Fig. S7. Zeta potential of N-Cdots (dissolved in ultrapure water).

1. Quantum yield and fluorescence lifetime of N-Cdots

Quinine sulfate dissolved in 0.1 M H_2SO_4 (with the known quantum yield of 0.54 at 360 nm) was chosen as a standard to calculate the quantum yield of N-Cdots with the following equation:

$$\Phi_x=\Phi_{std}(I_x/I_{std})(\eta^2{}_x/\eta^2{}_{std})(A_{std}/A_x)$$

Φ stands for quantum yield, I is the measured integrated emission intensity, η is the refractive index, and A is the optical density. The subscript std refers to the referenced fluorophore with known quantum yield. In order to minimize re-absorption effects, absorption was kept below 0.05 at the excitation wavelength of 360 nm.

Table S1. Fluorescence quantum yield of N-Cdots

Sample	*I*	*Abs*	*η*	*QY*
Quinine sulfate	6780	0.043	1.33	0.54 (known)
N-Cdots	650.7	0.042	1.33	0.052

Table S2. Fluorescence lifetime value and relative content of N-Cdots

Param	Value/ns	Rel.%
τ1	1.18	12.70
τ2	4.29	59.80
τ3	11.9	27.50

$$\tau = \tau1\times12.70\ \% + \tau2\times59.80\ \% + \tau3\times27.50\ \% = 7.26\ \text{ns}$$

So the fluorescence lifetime of the N-Cdots we synthesized is 7.26 ns.

2. Detection of Ag^+

We found the fluorescence of N-Cdots was quenched by Ag^+ ions. Then we evaluated the capability of N-Cdots for quantitative detection of Ag^+. As shown in Fig. S8a, the fluorescence intensity of the N-Cdots decreases gradually with the increasing concentrations of Ag^+, indicating that addition of Ag^+ can quench the fluorescence of N-Cdots effectively. A concentration-dependent emission was observed. As shown in Fig. S8b, a linear relationship between the fluorescence intensity and the concentration of Ag^+ was observed. So, the N-Cdots can be used to detect Ag^+ ions. The quenching mechanism of the N-Cdots by Ag^+ was investigated. The surface states of Cdots can be influenced by metal ions which can decrease the fluorescence intensity of the Cdots. [1] In the present of catechol group, Ag^+ ions are readily absorbed onto the surface of N-Cdots by the metal-catechol interaction.[2] The little shifts of emission peak from 536 nm to 521 nm in the fluorescence spectrum and reveals the variation of the surface states of N-Cdots after added with Ag^+ ions. The results suggest that Ag^+ ions change the surface state of N-Cdots to quench the fluorescence of N-Cdots.

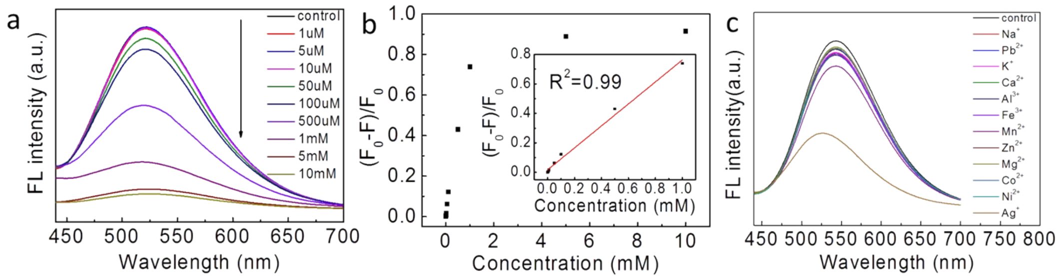

Fig. S8. (a) The fluorescence spectra of N-Cdots adding Ag^+ concentrations (0-10mM), (b) The relationship between the FL intensities of N-Cdots-Ag^+ (inset: the Ag^+ concentration from 0-1mM). (c)The fluorescence spectra of N-Cdots added with 500 μM metal ions.

3. Selectivity for Ag^+

To verify the special interaction between Ag^+ and N-Cdots, we tested the response of the N-Cdots towards other metal ions (Na^+, Pb^{2+}, K^+, Ca^{2+}, Al^{3+}, Fe^{3+}, Mn^{2+}, Zn^{2+}, Mg^{2+}, Co^{2+} and Ni^{2+}). Fig. S8c reveals that the fluorescence quenching to other metal ions is relatively weaker, which means the excellent selectivity of N-Cdots towards Ag^+.[3] As illustrated in the FTIR and XPS spectra, large amount of hydroxyl, amino and carboxyl groups distribute on the surface of the N-Cdots. The fluorescence quenching of N-Cdots may be caused by the surface states change of the N-Cdots which can be attributed to the affinity between the catechol groups on the surface of the N-Cdots and Ag^+ and the charge transfer process. The results reveals that catechol groups distributed on the surface of the N-Cdots which makes the N-Cdots applied in the detection of Ag^+ ions.

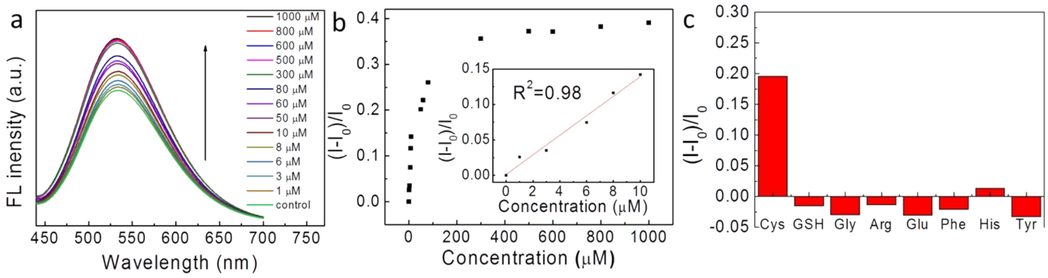

Fig. S9. (a) The fluorescence spectra of N-Cdots-Ag^+ adding cysteine with different concentrations (0-1000 μM), (b) The relationship between the FL intensities of N-Cdots-Ag^+ and the concentration of cysteine (inset: the concentration range of 0-10 μM). (c) The fluorescence response of the N-Cdots-Ag^+ system to 100 μM cysteine and other biological thiol group compounds.

4. Detection of cysteine

We also explored the sensing application of the N-Cdots-Ag^+ platform for cysteine by the competition interaction. Cysteine has a thiol group on the anomeric carbon, which is apt to interact with Ag^+ by the formation of Ag^+-S bond. [4] Moreover, the affinity between Ag^+ and cysteine is confirmed to be stronger than the metal-catechol interaction between Ag^+ and N-Cdots. [5] So the addition of cysteine into the N-Cdots-Ag^+ system can recover the N-Cdots fluorescence by the release of Ag^+ ions. The detection of cysteine was therefore achieved by taking use of the affinity between Ag^+ and cysteine. The fluorescence spectra obtained from different concentration of cysteine are recorded in Fig. S9a. As expected, the fluorescence intensity was enhanced effectively with the cysteine concentration increasing. Fig. S9b shows the fluorescence intensity as the function of the cysteine concentration. The linear relationship between the fluorescence intensity and the cysteine concentration was observed in the 0-10 μM as shown in the inset of Fig. S9b. So, the N-Cdots-Ag^+ system can be applied for the detection of cysteine.

5. Selectivity for cysteine

The specificity of the N-Cdots-Ag^+ system for cysteine was investigated. The possible interference may come from some biological thiol compounds such as GSH, L-histidine, lysine, L-arginine, L-glutamate, L-phenylalanine, L-tyrosine and glycine. As shown in Fig. S9c, the N-Cdots-Ag^+ system shows stronger response to cysteine than the other species in 10 mM PBS buffer (pH 7.0). The results suggest the reliability and selectivity of the N-Cdots-Ag^+ system for detecting cysteine.

The affinity of cysteine towards Ag^+ has been reported and is stronger obviously than the electrostatic interaction between N-Cdots and Ag^+.[5] The interaction between cysteine and Ag^+ partly reduce the interaction between N-Cdots and Ag^+, which leads to the recovery of the fluorescence signal of N-Cdots, as illustrated in Fig. S9a. The sensing strategy was applied to analyze the bovine serum samples to evaluate the feasibility of the proposed method. Two diluted bovine serum samples were chose to test quantitative recovery of the spiked cysteine. The concentrations of the cysteine contained in the serum and the spiked solution were shown in Table S3, where the recoveries of cysteine were found between the 106.40-103.33%. The results further demonstrated the feasibility of the sensing of N-Cdots-Ag to the cysteine.

Table S3. Determination of cysteine in bovine serum samples.

Diluted sample	Determined cysteine/mM	Added cysteine/mM	Measured/mM	Recovery(%)	RSD(%,n=3)
Serum 1	7.21	15	22.71	103.33	4.05
Serum 2	14.63	15	30.59	106.40	1.70

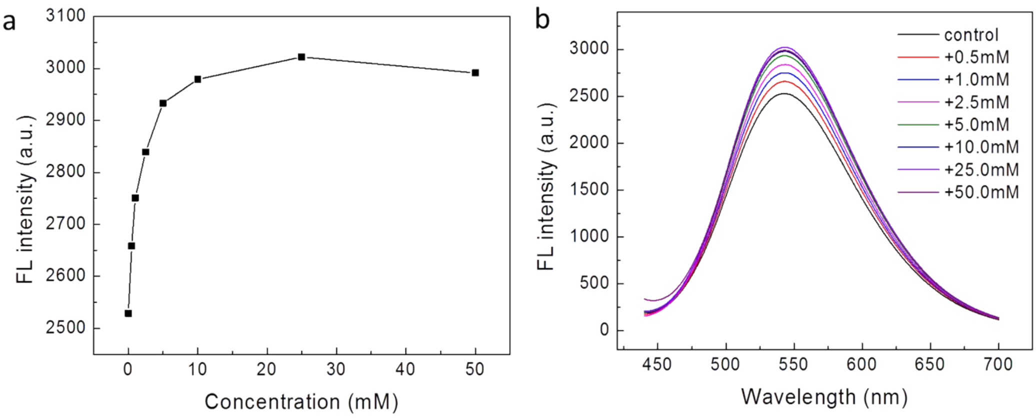

Fig. S10. The FL intensity (a) and fluorescence spectra (b) of N-Cdots (0.125 mg mL^{-1} dissolved in 10 mM pH=8.5 PBS) treated with different concentration of H_3BO_3 solution.

6. Cytotoxicity of N-Cdots

Cytotoxicity of N-Cdots was quantitatively measured with A549 cells by flow cytometry. As presented in Fig. S11, the cytotoxicity of N-Cdots was rather low with the mortality rate of 4.20 % at high concentration of 1.0 mg mL^{-1}. The mortality rate of cells after incubated with different concentration (0.6, 0.8, 1.0 mg mL^{-1}) of N-Cdots present no significant difference. In Fig. S12, Q4, Q3, Q1 and Q2 represent to the percentage of non-apoptotic cells, early apoptotic cells, terminal apoptotic cells and necrotic cells. As shown in Fig. S12 and Table S4, after incubated with 0.6, 0.8, 1.0 mg mL^{-1} N-Cdots, most of the A549 cells (average value: 80.1%) are at no apoptotic cell and early apoptotic cell stage. And the percentage of early apoptotic cells after incubated with different concentration of N-Cdots present no significant difference. All of the results confirm the low cytotoxicity and high bio-compatibility of N-Cdots we synthesized.

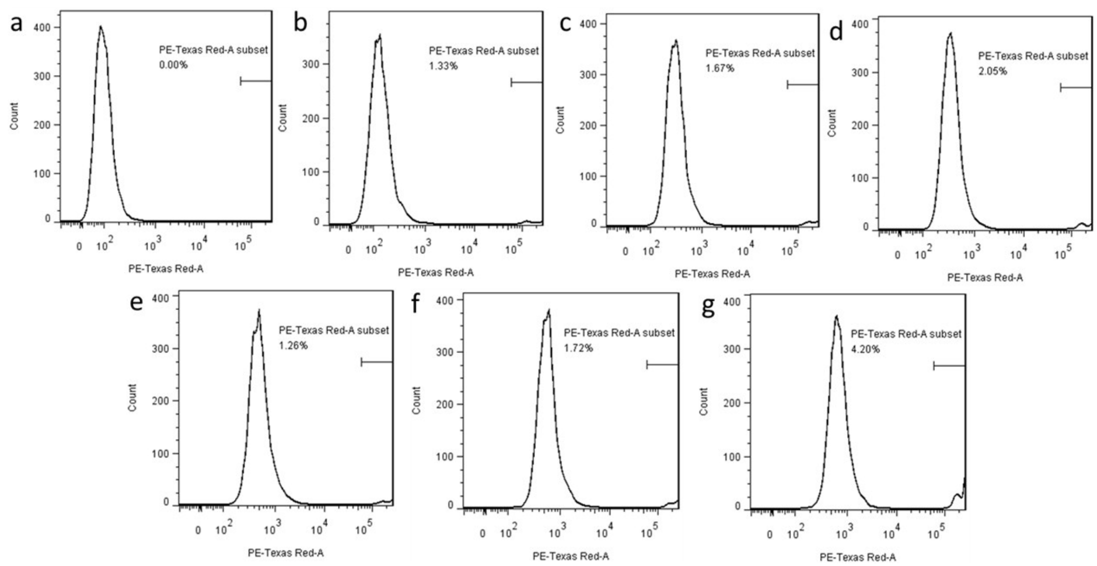

Fig. S11. Cytotoxicity of N-Cdots towards A549 cells measured by flow cytometry. (a) negative control used for select "gate" and A549 cells were incubated with (b) 0 (control), (c) 0.2, (d) 0.4,(e) 0.6, (f) 0.8, and (g) 1.0 mg mL^{-1} of N-Cdots for 12 h, respectively. The A549 cells were stained with PI.

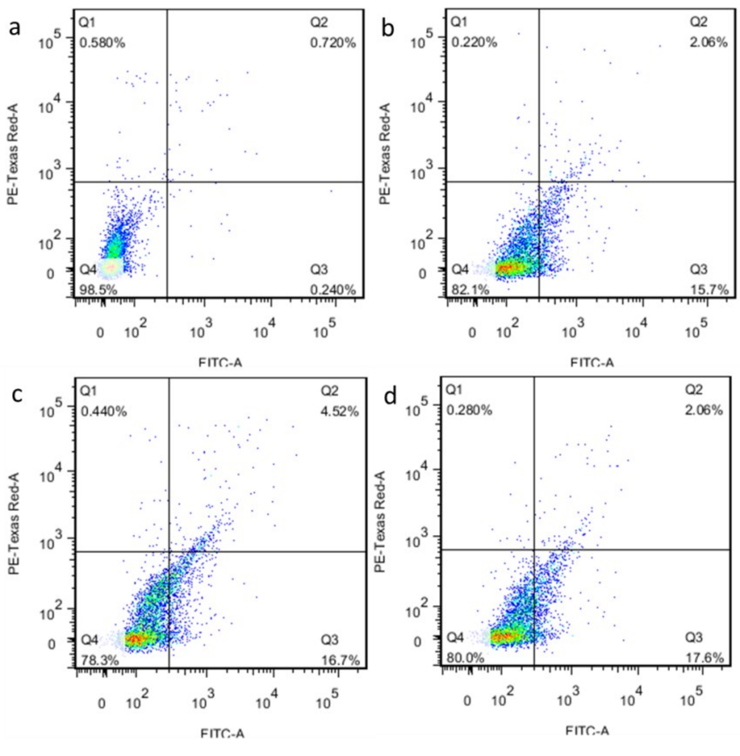

Fig. S12. Cytotoxicity of N-Cdots towards A549 cells measured by flow cytometry. A549 cells were incubated with (a) 0 (positive control used for select "gate"), (b) 0.6, (c) 0.8, and (d) 1.0 mg mL^{-1} of N-Cdots for 12 h. The A549 cells were stained with Annexin V-FITC and PI.

Table S4. The distribution of A549 cells in different stages after incubated with 0, 0.6, 0.8 and 1.0 mg mL^{-1} of N-Cdots for 12 h measured by flow cytometry. The percentage of Q4, Q3, Q1 and Q2 is related to the non-apoptotic cells, early apoptotic cells, terminal apoptotic cells and necrotic cells. The results come from Fig. S12.

Sample	Q4	Q3	Q1	Q2
0 mg mL^{-1}	98.5%	0.240%	0.580%	0.720%
0.6 mg mL^{-1}	82.1%	15.7%	0.220%	2.06%
0.8 mg mL^{-1}	78.3%	16.7%	0.440%	4.52%
1.0 mg mL^{-1}	80%	17.6%	0.280%	2.06%
Average*	80.1%	16.7%	0.313%	2.88%

* The average represents the average percentage results from 0.6, 0.8, 1.0 mg mL^{-1} samples.

Reference

1. L. Zhou, Y.-H Lin, Z.-Z. Huang, J.-S. Ren and X.-G. Qu, *Chem. Commun.*, 2012, **48**, 1147-1149.
2. Y. H. Lin, C. E. Chen, C. Y. Wang, F. Pu, J. S. Ren and X. G. Qua, *Chem. Commun.*, 2011, **47**, 1181–1183.
3. S. J. Jeon, S. Y. Kwak, D. Yim, J. M. Ju and J. H. Kim, *J. Am. Chem. Soc.,* 2014, **136**, 10842-10845.
4. S. N. Baker and G. A. Baker, *Angew. Chem. Int. Ed. Engl.*, 2010, **49**, 6726-6744
5. L. C. Gruen, *Biochim. Biophys. Acta*, 1975, **386**, 270-274.